

Available at www.sciencedirect.comjournal homepage: www.elsevier.com/locate/he

Synthesis and characterization of colloidal platinum nanoparticles for electrochemical applications

B. Escobar Morales^a, S.A. Gamboa^a, U. Pal^b, Rene Guardián^c, D. Acosta^d, Carlos Magaña^d, X. Mathew^{a,*}

^aCentro de Investigación en Energía, Universidad Nacional Autónoma de México, Temixco, Morelos 62580, México

^bInstituto de Física, Universidad Autónoma de Puebla, Puebla, México

^cInstituto de Ciencias Físicas, Cuernavaca, Morelos, México

^dInstituto de Física, Universidad Nacional Autónoma de México, D.F., México

ARTICLE INFO

Article history:

Received 24 June 2009

Received in revised form

8 January 2010

Accepted 13 January 2010

Available online 12 March 2010

Keywords:

Pt nanoparticles

PEM fuel cell

Oxygen reduction reaction

Exchange current density

Tafel

HRTEM

ABSTRACT

Platinum colloidal nanoparticles were synthesized by chemical reduction of metallic salts in presence of poly (N-vinyl-2-pyrrolidone) which served as a protecting agent. The preparation conditions for obtaining Pt nanoparticles were established by analyzing TEM and HRTEM images of the samples. Size of the synthesized Pt nanoparticles was in the range 2.5 to 8.5 nm depending on the molarity of PtCl₄ used to prepare the colloidal dispersion. The electrochemical characteristics of the Pt nanoparticles supported on carbon were investigated by analyzing their catalytic response to the oxygen reduction reaction (ORR). The reactivity of the prepared catalyst was comparable to that of the commercially available carbon supported Pt for the ORR. Catalytic parameters like charge transfer coefficient, Tafel constants and exchange current density were calculated for the prepared catalyst.

© 2010 Professor T. Nejat Veziroglu. Published by Elsevier Ltd. All rights reserved.

1. Introduction

The development of new nanostructured materials with optimal physicochemical characteristics for specific scientific and technological applications has necessarily promoted the use of chemical methods which can obtain materials with good control on particle size and distribution. Good quality colloidal nanoparticles are produced by thermal [1], photochemical [2], electrochemical [3] and chemical reduction methods [4–7].

The preparation of colloidal nanoparticles by chemical reduction has been recently investigated and this method has proved the feasibility to obtain well dispersed carbon

supported catalyst [8,9]. The method is based on the reduction of the corresponding metallic ions in aqueous solution in presence of a stabilizer. Carbon supported nanostructured catalysts have recently been investigated in chemical and electrochemical systems to correlate their physicochemical properties like particle size, distribution, chemical composition, and the influence of structure on their catalytic performances [10–14]. There are many technical reports indicating the use and evaluation of metallic catalysts obtained by chemical methods in industrial applications due to their adequate catalytic activity and stable performance [15,16]. The growth of nanometric particles is achieved by the reduction of metallic ions in presence of different solvents

* Corresponding author. Tel.: +52 55 562 29720; fax: +52 777 325 0018.

E-mail address: xm@cie.unam.mx (X. Mathew).

0360-3199/\$ – see front matter © 2010 Professor T. Nejat Veziroglu. Published by Elsevier Ltd. All rights reserved.

doi:10.1016/j.ijhydene.2010.01.040

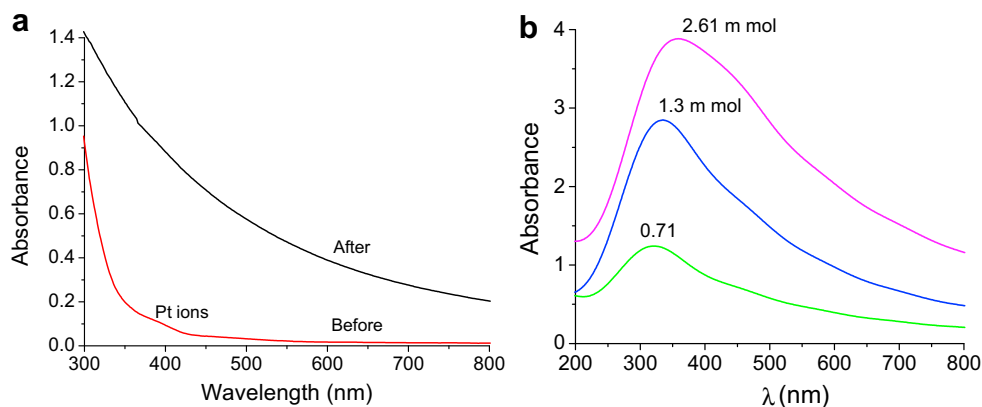


Fig. 1 – Optical absorption spectra of (a) colloidal dispersions of Pt before and after the reduction process; and (b) absorption spectra of the colloidal dispersions of Pt prepared at different precursor concentrations.

and organic materials as ligands or surfactants. Several factors like stabilizer, reducing agent and solvent have been modified to control the size of the particles. With the previously mentioned methods it is possible to control the size of the metallic particle but not the crystallographic orientation. Nevertheless, the synthesis of the nanoparticles with good dispersion is a first step followed by supporting these colloidal dispersions on carbon. Carbon supported Pt nanoparticles is one of the important components in the membrane electrode assembly (MEA) of proton exchange membrane (PEM) fuel cells. Pt is proven to be the best catalyst for both oxidation and reduction reactions, however high material cost is a major concern in the large scale production of MEAs. One way to overcome this is to use nano-sized catalyst, which can reduce the quantity of material due to the availability of large active surface area. We have prepared Pt nanoparticles by a wet chemical method and studied by TEM and optical absorption spectroscopy. In analytical chemistry, the color of the dispersed solution is important since it is related to the size of the particles which absorb the light [17,18]. TEM can provide indirect information of the atomic arrangements of the nanoparticles. The oxygen reduction rate of the prepared electrodes was studied by rotating disc electrochemical methods [19–22].

2. Synthesis and characterization of the monometallic Pt nanoparticles

For the preparation of colloidal dispersions of Pt nanoparticles, different amounts of platinum tetrachloride were dispersed in methanol (0.71, 1.3 and 2.61 m mol). 75 mg of poly (*N*-vinyl-2-pyrrolidone) (PVP) was added to 25 ml of the metal ion solution as the capping agent. A stable homogeneous dark brown colored colloidal dispersion was formed after adding NaBH_4 (1 ml of the 0.044 m mol solution).

A Shimadzu model UV1601 double beam spectrophotometer was used to measure the absorption spectra of the colloids in the range 300–800 nm. A typical absorption spectrum of a metal ion solution before and after the addition of

reducing agent (NaBH_4) is presented in Fig. 1a. Absorption spectrum of the colloidal solutions prepared with different metal ion concentrations are presented in Fig. 1b. The absorption spectra prior to the addition of reducing agent show an absorption shoulder in the region 350–400 nm which is characteristic of the platinum ions [6,11].

3. Results and discussion

3.1. UV–VIS absorption spectra

The colloidal dispersions of platinum nanoparticles in presence of PVP after reduction do not exhibit any characteristic peak in their absorption spectrum (Fig. 1a), indicating the complete reduction of Pt ions to metallic atoms. The change in color of the solution from pale yellow to dark brown after the addition of reducing agent indicates the formation of nanometric particles. The changes in the absorption and in the color imply a change in the colloidal properties [23]. The increase in the absorbance towards shorter wavelengths (Fig. 1b) with the increase of metal ion concentration is in agreement with the previous reports [6,24].

3.2. TEM analysis

The size and shape of the platinum particles were determined from TEM analysis. For TEM study, a drop of colloidal sample was dispersed on a carbon coated microscopic grid and dried in vacuum. The average particle size was obtained by measuring the diameter of a sufficient number of particles and plotting their size distribution histogram. Typical TEM micrographs of the Pt nanoparticles with three different concentrations of the precursor solutions are shown in Fig. 2. Size distribution histograms of the corresponding nanoparticles are given beside their TEM micrographs (Fig. 2). From the histograms presented Fig. 2; the average size of the particles was estimated at 8.5, 4.5 and 2.7 nm for the precursor concentration of 2.61 m mol, 1.3 m mol and 0.71 m mol, respectively. The TEM images revealed the formation of Pt

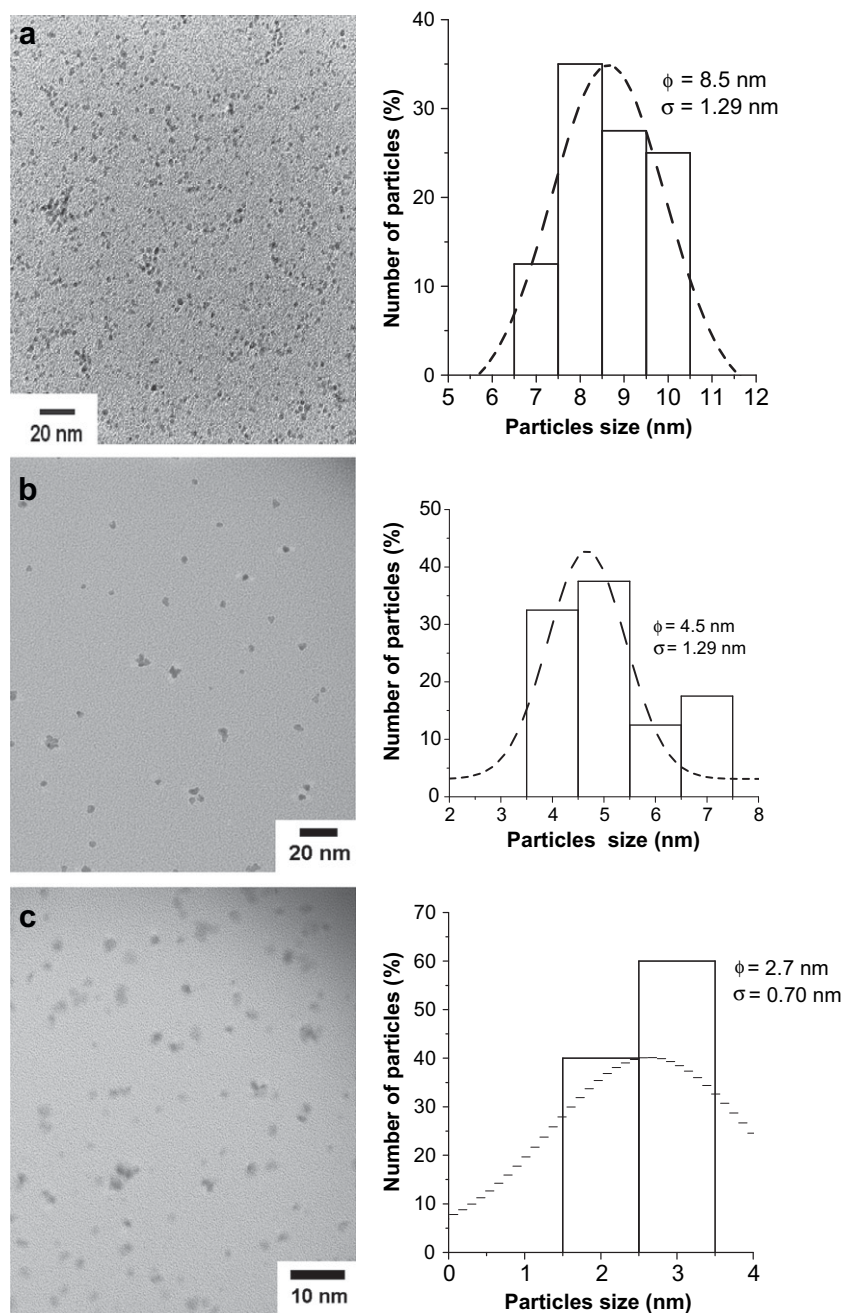


Fig. 2 – TEM micrograph of platinum particles with (a) 2.61 m mol of PtCl_4 , (b) 1.3 m mol of PtCl_4 , (c) 0.71 m mol of PtCl_4 in the reaction mixture. Corresponding particle size distribution histograms are presented alongside.

particles of spherical shape with increasing size on increasing the concentration of the precursor as reported in literature [25]. As can be seen from Fig. 2, the Pt nanoparticles prepared with higher concentrations of the metal precursor are partially agglomerated. This indicates that the amount of PVP should be increased with the increase of metal precursor in the reaction solution to obtain well dispersed particles. In order to determine the form and structure of the obtained nanoparticles, HREM analysis was carried out. Fig. 3 shows typical HREM image of the particles of about 2.5 nm sizes with almost perfect lattice planes of cubic fcc structure.

4. Electrochemical characterization

4.1. Synthesis and preparation of electrodes

The carbon supported Pt catalyst was prepared by mixing 2 mg of carbon in 0.3 ml of hydrogen peroxide and allowed to dry. Later 1 ml of the colloidal dispersion prepared with 2.61 m mol of PtCl_4 was added to this while continuing the drying process. The resulting powder was annealed for 20 minutes at 330 °C in N_2 atmosphere. Finally the baked powder was pulverized and

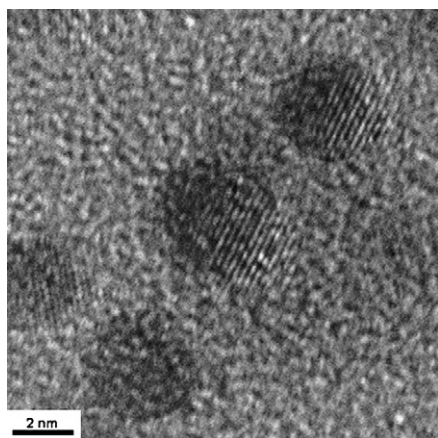


Fig. 3 – Typical high resolution TEM images of the Pt nanoparticles synthesized by wet chemical method. Crystallinity of the nanoparticles is clear from the well ordered lattice planes.

mixed with isopropanol and Nafion solution in an ultrasonic agitator. Five micro liter of the above ink was deposited onto the rotating disk electrode. Different electrodes were prepared with three sets of nanoparticles dispersions prepared with 2.61, 1.3 and 0.71 m mol PtCl₄.

4.2. Cyclic voltamperometry

Cyclic voltammetry measurements were carried out at a sweeping speed of 30 mVs⁻¹ in inert atmosphere of

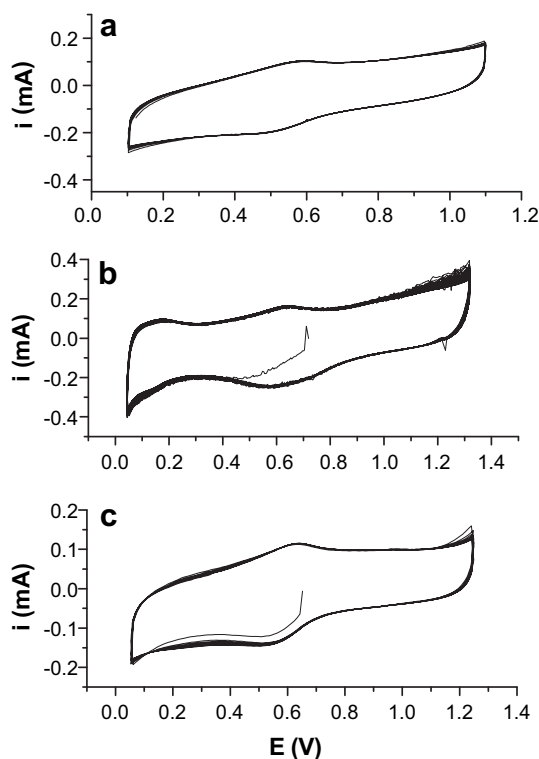


Fig. 4 – Cyclic voltammograms for the carbon supported platinum catalyst prepared with different amounts of PtCl₄: a) 0.71 m mol, b) 1.3 m mol and c) 2.61 m mol.

nitrogen. The electrolyte in all cases was 0.5 M H₂SO₄, and prior to the voltammetry measurements, the electrolyte was de-oxygenated by bubbling N₂ for 30 minutes. The cyclic voltammogram of the three electrodes are shown in Fig. 4. The peaks corresponding to the adsorption and desorption of hydrogen atoms as well as the region where monolayers of oxides are formed can be seen in Fig. 4. It was possible to observe the reversible hydrogen electrode performance associated to a metallic oxide, the H-adatoms adsorption and desorption are not observed symmetrically in the cyclic voltammetry for the Pt based catalysts supported on carbon, it was not proper to calculate specific areas from that mechanism and it is possible to assume that the process could be controlled by diffusion desorption processes in order to maintain similar charge capacity as function of cyclic scans. For simplicity, the specific surface areas were calculated from cathodic reactions.

The oxide formation occurs between 0.4 and 1.2 V while the reduction starts approximately at 1.0 V. Takasu et al. found that the position of hydrogen adsorption/desorption peak and the oxygen reduction peak changes with the average size of the particles [26–32]. It should be noticed that the increase in size of the Pt particle is proportional to the molarity of the colloidal dispersion, and as the particle size increases, the oxygen reduction peak becomes well defined indicating that a change happens with the size of the particles in the electrode. This effect is more pronounced in Fig. 4b and c. There are different observations reported in literature in this respect; some reports say that the specific activity decreased and the slope of Tafel plot increased with the decrease in particle size [26–30], but some reports show different results [31,32]. Watanabe et al. discussed that the effect of the particle size is not truly dependant on the dimensions of the Pt crystallites but it is dependant on the inter-crystalline distance [32]. According to this hypothesis, the specific activity was also increased with the decrease in the size of the platinum particle when the separation of the crystals is less than 18 nm. On the other hand, Kinoshita et al. have observed that the specific activity diminishes steeply with the decrease in the size of the particles [27–30].

4.3. Oxygen reduction reaction

Fig. 5 shows hydrodynamic voltammograms for the ORR at the platinum working electrode in O₂ saturated 0.5 M H₂SO₄, at a sweeping rate of 5 mVs⁻¹ and with rotation speed in the range of 100 rpm to 1800 rpm at of 25 °C. Fig. 5a and b shows the polarization curves obtained for the ORR for different catalyst concentrations, 0.71 m mol and 1.3 m mol PtCl₄ in the precursor solution respectively. An increase in current is observed as the rotation speed increases, until about 600 rpm, for higher rotation speeds the increase in current is not very significant. This type of behavior, where the current increases significantly until arriving to a certain rotational speed is attributed to processes of mixed control, is to say, convection and diffusion process, while the graphs for which the current is independent of the speed of rotation is attributed to the processes of activation [26]. The polarization curves obtained for the catalyst samples prepared with of 2.61 m mol PtCl₄ is shown in Fig. 5c. It can be observed

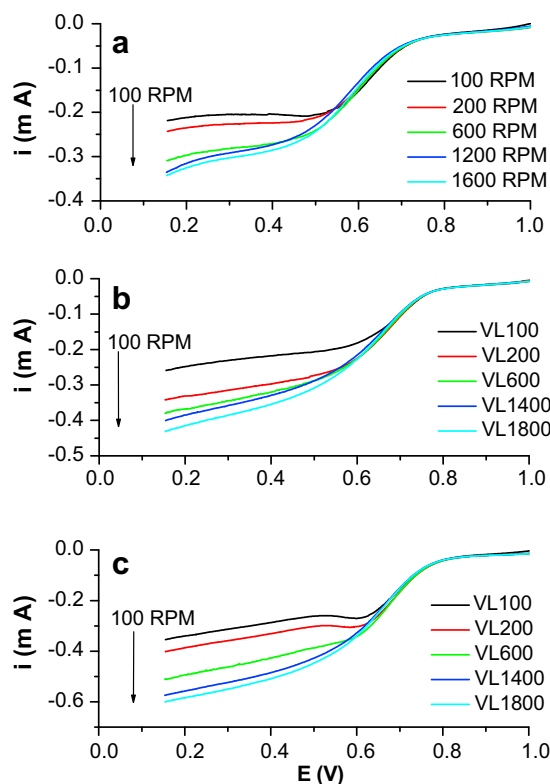


Fig. 5 – Polarization curve of oxygen reduction on the rotating disk electrode prepared with a) 0.71 m mol, b) 1.3 m mol, and c) 2.61 m mol of $PtCl_4$.

that the ORR potential shows a cathodic displacement and an increase in current. It can be noted that at high rotation speeds the polarization curves of oxygen reduction appear inclined, this phenomenon is associated with an irreversible process happened at the electrode when the catalyst is impregnated on the electrode [33]. The results of the calculations of the different electrochemical parameters of the Pt catalyst prepared with different molar concentrations of $PtCl_4$ in the precursor solution are shown in Tables 1–3.

The electrochemically active surface area was calculated in the kinetic region for the oxygen reduction reaction using the

Table 1 – Electrochemical parameters of the sample prepared with 0.71 m mol of $PtCl_4$.

| RPM | Tafel slope | i_0 | n_α |
|---------|-------------|----------|------------|
| 100 | 0.207 | 0.000160 | 0.284 |
| 200 | 0.215 | 0.000192 | 0.274 |
| 400 | 0.216 | 0.000199 | 0.273 |
| 600 | 0.219 | 0.000215 | 0.269 |
| 800 | 0.226 | 0.000252 | 0.260 |
| 1000 | 0.228 | 0.000256 | 0.258 |
| 1200 | 0.243 | 0.000342 | 0.242 |
| 1400 | 0.244 | 0.000354 | 0.242 |
| 1600 | 0.244 | 0.000369 | 0.242 |
| Average | 0.226 | 0.000259 | 0.260 |

Table 2 – Electrochemical parameters of the sample prepared with 1.3 m mol of $PtCl_4$.

| RPM | Tafel slope | i_0 | n_α |
|---------|-------------|----------|------------|
| 100 | 0.178 | 0.000108 | 0.331 |
| 200 | 0.179 | 0.000114 | 0.328 |
| 400 | 0.183 | 0.000134 | 0.322 |
| 600 | 0.188 | 0.000148 | 0.314 |
| 800 | 0.188 | 0.000151 | 0.314 |
| 1000 | 0.193 | 0.000173 | 0.305 |
| 1200 | 0.197 | 0.000192 | 0.299 |
| 1400 | 0.198 | 0.000196 | 0.298 |
| 1800 | 0.198 | 0.000197 | 0.298 |
| Average | 0.189 | 0.000157 | 0.312 |

experimental Koutecky–Levich slope. The equation used for this calculation is:

$$A_{EA} = \frac{1}{0.2nFB_{K-L}v^{-1/6}C_{O_2}D_{O_2}^{2/3}} \quad (1)$$

where n is the number of electrons transferred ($n=4$), F is Faraday constant ($F=96485$ C/mol), B_{K-L} is the experimental Koutecky–Levich slope, v is the kinematic viscosity ($v=0.01$ cm²/s), C_{O_2} is the Oxygen concentration close to the electrode surface ($C_{O_2}=1.1 \times 10^{-6}$ mol/cm³), and D_{O_2} is the oxygen diffusion coefficient ($D_{O_2}=1.4 \times 10^{-5}$ cm²/s). The specific surface area for the three Pt based catalysts ((a) 2.61 m mol of $PtCl_4$, (b) 1.3 m mol of $PtCl_4$, (c) 0.71 m mol of $PtCl_4$) was estimated at 0.042, 0.066 and 0.0071 cm², respectively. The active surface area can also be determined from the UPD H-adatoms desorption peaks provided the particle size is below 2 nm [34]. However, in the present case the particle size is larger than 2 nm and hence we didn't adopt this method.

We have intended to associate the size of the platinum particles in the electrode with respect to the change in their electrochemical properties. From the tables it is possible to observe that the Tafel slope (b) is increased with the decrease in the size of the particle, similar observation was reported by Takasu and collaborators [26]. In the present case, the samples show an increase in the slope of Tafel and in the exchange current density as the speed of rotation of the EDR increases, while the coefficient of mass transfer shows a decrease in its value conforms to the increase in the number of revolutions per minute.

Table 3 – Electrochemical parameters of the sample prepared with 2.61 m mol of $PtCl_4$.

| RPM | Tafel slope | i_0 | n_α |
|---------|-------------|----------|------------|
| 100 | 0.166 | 0.000105 | 0.353 |
| 200 | 0.167 | 0.000116 | 0.352 |
| 400 | 0.168 | 0.000117 | 0.350 |
| 600 | 0.169 | 0.000122 | 0.349 |
| 800 | 0.169 | 0.000121 | 0.348 |
| 1000 | 0.172 | 0.000131 | 0.343 |
| 1200 | 0.173 | 0.000131 | 0.340 |
| 1400 | 0.173 | 0.000134 | 0.340 |
| 1600 | 0.174 | 0.000134 | 0.339 |
| 1800 | 0.174 | 0.000140 | 0.338 |
| Average | 0.170 | 0.000125 | 0.345 |

5. Conclusions

We have synthesized Pt nanoparticles with size in the range 2.5 to 8.5 nm. The electrochemical characteristics of the prepared Pt nanoparticles were investigated by analyzing the response of the nanostructured catalyst to the oxygen reduction reaction. The reactivity of our carbon supported catalyst was comparable to that of the commercially available carbon supported Pt for the oxygen reduction reaction. Catalytic parameters like charge transfer coefficient, Tafel constants and exchange current density were calculated for the prepared catalyst.

Acknowledgements

B.E. Morales acknowledges the scholarship received from CONACYT and DGEP for the Ph.D program. This work was partially supported by the project PAPIIT-UNAM-IN 118409.

REFERENCES

- [1] Shimizu T, Teranishi T, Hasegawa S, Miyake M. Size evolution of alkanethiol-protected gold nanoparticles by heat treatment in the solid state. *J Phys Chem B* 2003;107: 2719–24.
- [2] Meltzer S, Resch R, Koel B, Thompson M, Madhukar A, Requicha A, et al. Fabrication of nanostructures by hydroxylamine seeding of gold nanoparticle templates. *Langmuir* 2001;17:1713–8.
- [3] Vracar M, Krstajic N, Radmilovic V, Jaksic M. Electrocatalysis by nanoparticles – oxygen reduction on Ebonex/Pt electrode. *J Electroanal Chem* 2006;587:99–107.
- [4] Du YK, Yang P, Mou ZG, Hua NP, Jiang L. Thermal decomposition behaviors of PVP coated on platinum nanoparticles. *J Appl Polym Sci* 2006;99:23–6.
- [5] Wang H, Qiao X, Chen J, Wang X, Ding S. Mechanisms of PVP in the preparation of silver nanoparticles. *Mater Chem Phys* 2005;94:449–53.
- [6] Duff DG, Edwards PP, Johnson FG. Formation of a polymer-protected platinum sol: a new understanding of the parameters controlling morphology. *J Phys Chem* 1995; 99:15934–44.
- [7] Zeng J, Yang JL, Zhou W. Activities of Pt/C catalysts prepared by low temperature chemical reduction methods. *Appl Catal A* 2006;308:99–104.
- [8] Wu C, Mosher BP, Zeng T. Rapid synthesis of gold and platinum nanoparticles using metal displacement reduction with sonomechanical assistance. *Chem Mater* 2006;18: 2925–8.
- [9] Shim J, Yeon KJ, Hwan JA, Moo WL. Carbon-supported platinum nanoparticles synthesized by plasma-chemical reduction method for fuel cell applications. *J Electrochem Soc* 2007;154:B165–9.
- [10] Yang J, Yang JL, Heng-Phon T. Size sorting of Au and Pt nanoparticles from arbitrary particle size distributions. *Anal Chim Acta* 2005;546:133–8.
- [11] Zhou M, Chen S, Ren H, Wu L, Zhao S. Electrochemical formation of platinum nanoparticles by a novel rotating cathode method. *Physica E* 2005;27:341–50.
- [12] Miyazaki A, Balint I, Nakano Y. Morphology control of platinum nanoparticles and their catalytic properties. *J Nanopart Res* 2003;5:69–80.
- [13] Tang Z, Geng D, Lu GT. Size-controlled synthesis of colloidal platinum nanoparticles and their activity for the electrocatalytic oxidation of carbon monoxide. *Mater Lett* 2005;59:1567–70.
- [14] Selvaraju T, Ramaraj R. Electrochemically deposited nanostructured platinum on Nafion coated electrode for sensor applications. *J Electroanal Chem* 2005;585:290–300.
- [15] Zen JM, Senthil A, Chung CR. A glucose biosensor employing a stable artificial peroxidase based on ruthenium purple anchored cinder. *Anal Chem* 2003;75:2703–9.
- [16] Hrapovic S, Luong JH. Picoamperometric detection of glucose at ultrasmall platinum-based biosensors: preparation and characterization. *Anal Chem* 2003;75:3308–15.
- [17] Teranishi T, Hosoe M, Tanaka T, Miyake M. Size control of monodispersed Pt nanoparticles and their 2D organization by electrophoretic deposition. *J Phys Chem B* 1999;103: 3818–27.
- [18] Bönemann H, Brijoux W, Siepen K, Hormes J, Franke R, Pollmann. Surfactant stabilized palladium colloids as precursors for cis-selective alkynehydrogenation catalysts. *Appl Org Chem* 1997;11:783–96.
- [19] Cezar-Salgado JR, Antolini E, González EF. Carbon supported Pt-Co alloys as methanol-resistant oxygen-reduction electrocatalysts for direct methanol fuel cells. *Appl Catal B Environ* 2005;57:283–90.
- [20] Wakabayashi N, Takeichi M, Itagaki M, Uchida H, Watanabe M. Temperature-dependence of oxygen reduction activity at a platinum electrode in an acidic electrolyte solution investigated with a channel flow double electrode. *J Electroanal Chem* 2005;574:339–46.
- [21] Koffi RC, Coutanceau C, Garnier E, Leger JM, Lamy C. Synthesis, characterization and electrocatalytic behavior of non-alloyed PtCr methanol tolerant nanoelectrocatalysts for the oxygen reduction reaction (ORR). *Electrochim Acta* 2005; 50:4117–27.
- [22] Gilman S. A study of the mechanism of carbon monoxide adsorption on platinum by a new electrochemical procedure. *J Phys Chem* 1963;67:78–84.
- [23] Yu-Hung C, Yao-Hung T, Chen-Sheng Y. Laser-induced alloying Au–Pd and Ag–Pd colloidal mixtures: the formation of dispersed Au/Pd and Ag/Pd nanoparticles. *J Mater Chem* 2002;12:1419–22.
- [24] Henglein A. Preparation and optical absorption spectra of AucorePtshell and PtcoreAushell colloidal nanoparticles in aqueous solution. *J Phys Chem B* 2000;104:2201–3.
- [25] Tang Z, Geng D, Lu G. Size-controlled synthesis of colloidal platinum nanoparticles and their activity for the electrocatalytic oxidation of carbon monoxide. *Mater Lett* 2005;59:1567–70.
- [26] Takasu Y, Ohashi N, Zhang XG, Murakami Y, Minagawa H, Sato S, et al. Size effects of platinum particles on the electroreduction of oxygen. *Electrochim Acta* 1996;41: 2595–600.
- [27] Satter ML, Ross PN. The surface structure of Pt crystallites supported on carbon black. *Ultramicroscopy* 1986;20:21–8.
- [28] Peuckert M, Yoneda T, Dalla RA, Boudart M. Oxygen reduction on small supported platinum particles. *J Electrochem Soc* 1986;133:944–7.
- [29] Kinoshita K. Particle size effects for oxygen reduction on highly dispersed platinum in acid electrolytes. *J Electrochem Soc* 1990;137:845–8.
- [30] Passalacqua E, Lufano F, Squadrito G, Patti A, Giorgi L. Nafion content in the catalyst layer of polymer electrolyte fuel cells: effects on structure and performance. *Electrochim Acta* 2001;46:799–805.

-
- [31] Bett J, Lundquist J, Washintong E, Stonehart P. Platinum crystallite size considerations for electrocatalytic oxygen reduction—I. *Electrochim Acta* 1973;18:343–8.
- [32] Watanabe M, Uchida H, Emori M. Polymer electrolyte membranes incorporated with nanometer-size particles of Pt and/or metal-oxides: experimental analysis of the self-humidification and suppression of gas-crossover in fuel cells. *J Phys Chem B* 1998;102:3129–37.
- [33] Jian R, Chu D. Remarkably active catalysts for the electroreduction of O₂ to H₂O for use in an acidic electrolyte containing concentrated methanol. *J Electrochem Soc* 2000; 147:4605–9.
- [34] Krstajic NV, Vracar LM, Radmilovic VR, Neophytides SG, Labou M, Jacksic JM, et al. Advances in interactive supported electrocatalysts for hydrogen and oxygen electrode reactions. *Surf Sci* 2007;601:1949–66.